Complex H-bonded silanol network in zeolites revealed by IR and NMR spectroscopy combined with DFT calculations †

Eddy Dib, Izabel Medeiros Costa, Georgi N Vayssilov, Hristiyan A Aleksandrov, Svetlana Mintova

Complex H-bonded silanol network in zeolites revealed by IR and NMR spectroscopy combined with DFT calculations†

Received 00th January 20xx,
Accepted 00th January 20xx

DOI: 10.1039/x0xx00000x

Eddy Dib [a], Izabel Medeiros Costa [a], Georgi N. Vayssilov* [b], Hristiyan A. Aleksandrov [b] and Svetlana Mintova*[a]

The amount and location of acid sites (strong Brønsted and weak silanols) in zeolites are crucial for their applications. In this work we revealed the enigma of the complex H-bonded silanol networks in pure silica MFI-type zeolites using ^{1}H solid-state NMR and IR spectroscopy combined with DFT calculations. The silanol sites have a determining role in phase selectivity during the zeolite synthesis and also play an imperative role in setting their acidity, stability, lifetime and hydrophobicity. The spectral signatures of silanol defects in the pure silica zeolites are disclosed. Based on the experimental and theoretical observations we identified four types of silanols in the pure silica zeolites which varied dependent of the crystallite sizes: (i) isolated (free) silanols, not participating in hydrogen bonds either as proton-donors nor as proton-acceptors, (ii) proton-acceptor silanols, participating in hydrogen bonds only as proton-acceptor, (iii) proton-donor silanols, participating in weak hydrogen bonds and (iv) medium and strong hydrogen bonded silanols, participating as proton-donors or simultaneously as proton-donors and proton-acceptors. The main factor determining the strength of the hydrogen bond of a specific silanol group is the possibility its proton has to approach closer to the oxygen center of the proton accepting silanol. This suggested that the flexibility of the zeolite fragment at which the proton-donating and proton-accepting silanols are bound is the main factor determining the formation and strength of the hydrogen bonds and their corresponding spectral features.

The hydrogen bond (H-bond), discovered at the very beginning of the 20th century is still a subject undergoing intense study[1] and despite the appearance of several re-views in the literature, the definition is still broad because of the complexity and chemical variability of the systems studied. Various classifications of the hydrogen bonds have been suggested based on their strength assessed in terms of binding energy, hydrogen bonding distance, elongation of the X-H bond, etc. Three types of H-bonds were distinguished: (i) strong H-bonds, which are considered similar to covalent bonds; (ii) moderate H-bonds, dominated by electrostatic interactions; and (iii) weak H-bonds, accomplished mainly by van der Waals interactions (VdW).[1] Thus, the energy range for dissociation of hydrogen bonds covers an interval between 0.2 and 40 kcal.mol^{-1}.[2]

Hydrogen bonds are a common feature of solids containing hydroxyl groups and their characterization is of prime importance knowing their influence on the final properties of the matter. While for crystalline solids, diffraction techniques are commonly used to determine the atomic positions, hydrogen atoms cannot be localized using X-ray diffraction (XRD), this is due to absence of non-valence electron layer.[3] Alternatively, infrared (IR) and Nuclear Magnetic Resonance (NMR) spectroscopies have both become key methods to investigate hydroxyl groups in the zeolites since the vibrational modes as well as the NMR parameters and interactions are very sensitive to the hydroxyl groups configurations.[4,5] The most commonly used parameters to describe hydroxyl groups are the frequency of the O-H stretching vibration in IR or the associated proton chemical shifts in NMR.[6,7] Although these are basic parameters in both techniques, an ambiguity remains in the peaks assignments and this is mainly due to hydrogen bonding giving rise to bands' overlapping and broadening that prevent detailed analysis.

Zeolites constitute more than 40% of the total solid catalysts used for oil refining, petrochemical processing and organic synthesis. The tailored Brønsted - Lewis acidity and basicity of the zeolites is due to hydroxyl (OH) groups between aluminium and silicon atoms in their framework structures.[8,9] Tuning the amount and location of these acid sites is crucial for selectivity enhancement purposes of the catalysts.[10] In addition, other hydroxyl groups bound only to silicon centres, the so called silanols, exist in the zeolite structures and are known to be less acidic. The silanols appear in the zeolites because of a Si-O-Si bridge break and they can be terminal (at the external surface of the zeolite crystals) or internal (in the interior of the crystals). The silanols are often considered as structural defects, however, they can affect the phase selectivity during hydrothermal processes.[11] Also, they play an important role in setting the acidity, stability, lifetime and hydrophobicity of the

[a] *Laboratoire Catalyse & Spectrochimie, Normandie Univ, ENSICAEN, UNICAEN, CNRS, 14000 Caen, France.*
** E-mail: mintova@ensicaen.fr*

[b] *Faculty of Chemistry and Pharmacy, University of Sofia, 1126 Sofia, Bulgaria.*
** E-mail: gnv@chem.uni-sofia.bg*

†Electronic Supplementary Information (ESI) available: [details of any supplementary information available should be included here]. See DOI: 10.1039/x0xx00000x

catalysts.[12] Therefore, the Brønsted acid sites and the OH groups in zeolites are still attracting high attention and many efforts have been made to localize them.[13] Several important findings regarding the Brønsted acid sites in zeolites have been reported thanks to quantum chemical calculations, often based on the density functional theory method (DFT) in the last thirty years.[14-17] Recently, such calculations, combined with proton NMR and IR spectroscopy were used to understand the Brønsted acid sites (BAS) and their participation in hydrogen bonds in the ZSM-5 zeolites.[18-20] However, the precise assignment of the experimental spectra of hydroxyl groups in zeolites, both from NMR and IR spectroscopy, is very complicated due to line broadening and band overlapping. [21,22]

In this work, purposely we studied three pure silica zeolite samples in order to exclude the presence of BAS. Silicalite-1 samples with MFI type framework structure with different particle sizes are investigated with ^{1}H NMR and IR spectroscopy and DFT modelling in order to bring a rational methodology for the characterization of silanol defects and thus the assignment of their spectroscopic signatures. The three pure silica zeolites abbreviated as MFI-50, MFI-100 and MFI-2000 are standing for small (50 nm), average (100 nm) and big (2000 nm) crystals, respectively are shown in Figure 1. The zeolite crystals of samples MFI-50 and MFI-100 have spherical morphology while the MFI-2000 crystals have the typical coffin-like shape. The correspondent X-ray diffraction patterns of these samples are identical with the pattern theoretically predicted for pure MFI type zeolite.[23]

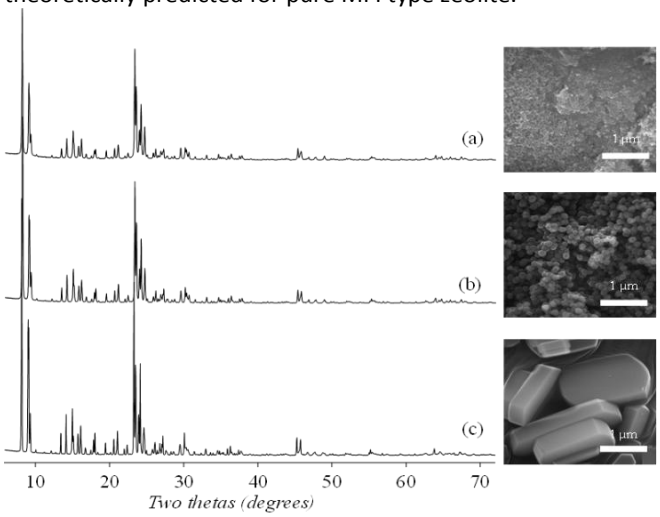

Figure 1. XRD patterns and SEM images of pure silica MFI type zeolites: (a) MFI-50, (b) MFI-100, and (c) MFI-2000 samples.

The different silanol groups of the three pure silica zeolites were characterized by IR, ^{29}Si and ^{1}H NMR (Figure 2). Depending on morphology and size of zeolite crystallites, different proportions of silanol are found. The ratio of Q^3/Q^4 species is evaluated based on the ^{29}Si NMR spectra: 3%, 7% and 14% Q^3 sites for samples MFI-50, MFI-100, and MFI-2000, respectively are found. Herein, Q^3 sites represent Si atoms bonded through oxygen bridges to three other Si atoms and one hydrogen ($(SiO)_3$-SiOH group), Q^4 sites represent Si atoms bonded through four oxygen bridges to four other Si atoms ($(SiO)_4$-Si group).[24] Several kinds of silanols covering a range from 1.8 to 5.8 ppm in the ^{1}H NMR and from 3740 to 3500 cm^{-1} in the IR spectra are revealed (Figure 2). These protons correspond to different silanols, some of them are involved in H-bonds (vide infra), keeping in mind that all samples are pure siliceous (silicalite-1) and they do not contain any aluminium and thus, no BAS are present. One may note here the superior resolution of the ^{1}H NMR spectra acquired at a rotation frequency of 40 kHz and their quantitative aspect when compared to IR spectra. The width of the peaks observed in the ^{1}H NMR spectra may be explained by a lower dipolar coupling of the low chemical shift protons, being more isolated than the higher chemical shift protons characterized by stronger H-bonding, then, stronger dipolar coupling. This latter results from the magnetic dipole-dipole interaction between the proton spins and is directly related to the distance between them.[25]

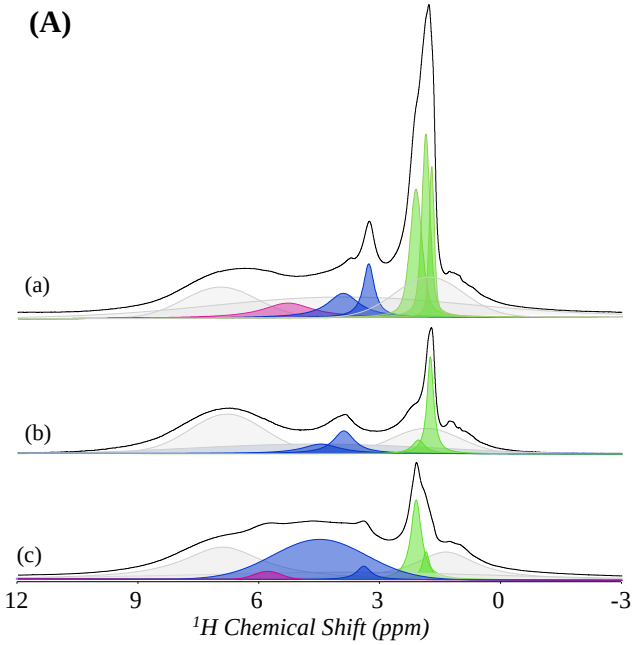

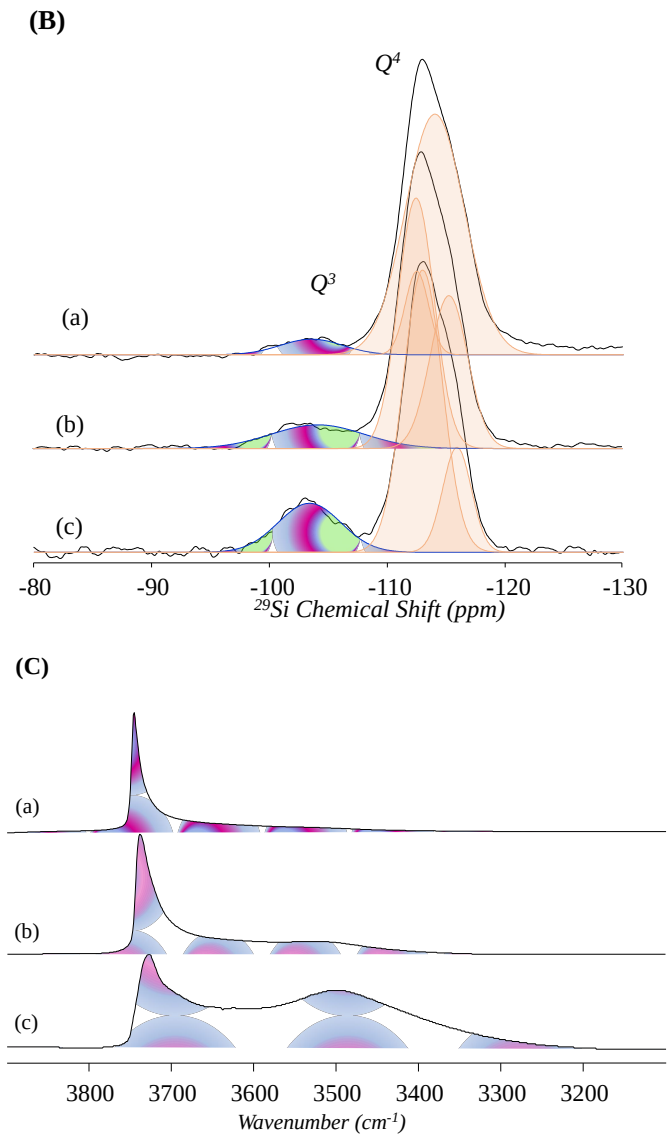

Figure 2. (A) ^{1}H NMR, (B) ^{29}Si NMR, (C) IR spectra of (a) MFI-50, (b) MFI-100, and (c) MFI-2000 zeolite samples. The gray peaks in the ^{1}H NMR deconvolution correspond to the vespel caps of the 1.9 mm rotors used. The experimental details and the fits are presented in Table S1, SI.

The spectral features of the zeolites experimentally measured are studied by computational modelling. This provides a unique way to accurately correlate both structural and spectral characteristics of individual silanol groups, and allows proper assignment of the specific types of silanols. For this reason, we performed quantum chemical calculations on four zeolite nanoparticle models using density functional theory (DFT) method. All calculations were performed with ORCA program package[26,27] with hybrid gradient-corrected PBE0 exchange-correlation functional. Further computational details are provided in Supporting Information (SI). The data for all silanol groups in the models (in total 130) were used to clarify the relation between the structure and bonding of silanols and their spectra.

The four zeolite models denoted as ZNP-99, ZNP-111, ZNP-165, ZNP-213, where the number corresponds to the total number of atoms in the models are presented in Table S2, SI. The models were obtained from the periodic MFI structure containing only Si in tetrahedral positions (T-atoms) as the fragments of the framework were cut at O-Si bonds and the dangling oxygen centers were saturated by hydrogen, thus forming silanol groups (Figure 3). The structures of the nanoparticles were optimized without any structural constraints. After optimization, their structures were preserved as in the periodic framework, and the changes affected mainly surface silanol groups and the corresponding Q^3 and Q^2 silicon centers in $(SiO)_3$-Si (OH) and $(SiO)_2$-Si-$(OH)_2$ groups, respectively.

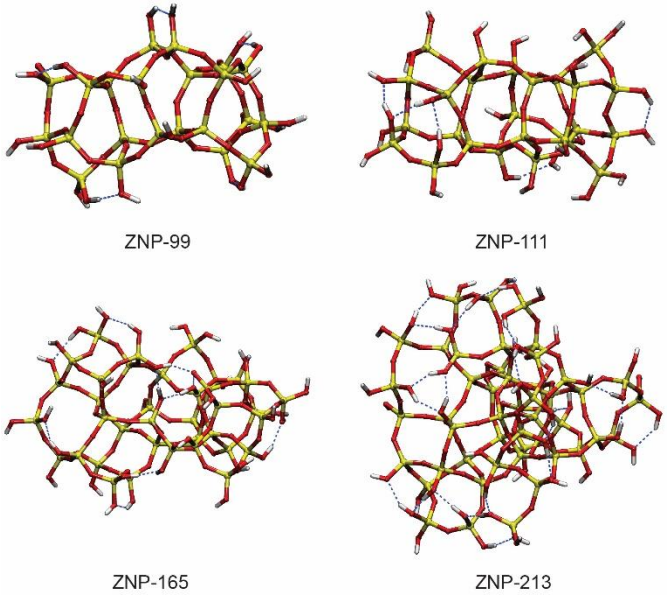

Figure 3. Optimized structures of the zeolite nanoparticles used for DFT calculations. All models contain only silicon T-atoms.

Several correlations between structural and spectral parameters of the silanol groups are considered: R(O-H) bond length in pm, H-O distance of hydrogen bond in pm where it exists, O-H stretching frequency (ν(O-H)) in cm^{-1} and ^{1}H NMR chemical shift (δ^{1}H) in ppm.

The absolute values of the O-H stretching frequency, ν(O-H) and ^{1}H NMR chemical shifts, δ^{1}H of all 130 simulated silanol groups were calculated, and the correlation is shown in Figure 4. This correlation holds for the whole interval of O-H frequency and chemical shifts, but cannot be applied for a narrow region, in particular for the silanols that do not participate in H-bonds as proton-donors. This is exemplified in Figure S1, where a closer view in the region between 1.2 and 2.0 ppm of the ^{1}H NMR spectrum is presented. The deviation in this region is due to perturbations from the completely isolated state caused by participation of the O-H group as proton-acceptor of H-bond, weak interactions with neighbouring zeolite framework or silanols. In this study,

based on computational results, obtained specifically for hydroxyl groups in silanols, we found δ^1H NMR = 44.6 – 0.0115 ν(O-H). This is in line with previous works of Brunner et al.[5,28] who obtained similar linear correlations between experimentally determined O-H stretching frequencies and ^{1}H NMR chemical shifts for different hydroxyl groups: δ^1H NMR = 57.1 – 0.0147 ν(O-H) for isolated hydroxyls and δ^1H NMR = 37.9 – 0.0092 ν(O-H) for H-bonded hydroxyls.

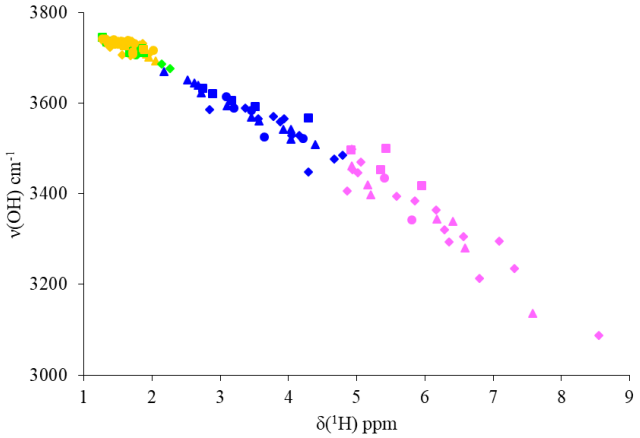

Figure 4. Correlation between calculated absolute values of the O-H stretching frequency and ^{1}H NMR chemical shift of the silanol groups in modeled zeolite nanoparticles: ZNP-99 (squares), ZNP-111 (circles), ZNP-165 (triangles), ZNP-213 (rhombus); ν(O-H) = 3868.3 – (84.989) δ^1H NMR (RMSD = 0.97). Tentative assignment of the data points corresponding to strong (pink), medium (blue), and weak (green) hydrogen bonds and non-interacting silanols (orange).

Both O-H stretching frequency and ^{1}H NMR chemical shift were found to correlate well with the R(O-H) bond length in the corresponding silanol. The relations are as follow: $\Delta(\delta^1H)$ = 2.2267 ΔR(O-H) (RMSD = 0.96); Δν(O-H) = -80.559 * $\Delta(\delta^1H)$ (RMSD = 0.97) and Δν(O-H) = -181.91 * ΔR(O-H) (RMSD = 0.98), where $\Delta(\delta^1H)$ corresponds to deviation with respect to reference values considered for non-interacting silanol group[29]: R(O-H) = 96.1 pm, δ^1H = 1.265 ppm, ν(O-H) = 3745 cm^{-1} (see SI for details). Based on these equations one can calculate tentatively the R(O-H) bond length from the measured vibrational frequency and the ^{1}H NMR chemical shift of a zeolite, or to predict the value of the O-H vibrational frequency from the measured ^{1}H NMR chemical shift as shown in Figure S2.

The connection between the hydrogen-bonded distance, R(H-bond), when the corresponding silanol group participates as proton-donor in a hydrogen bond and the three characteristics considered above is not linear, as the correlations, shown in Figure 4. Interestingly, a power relation between R(H-bond) and ^{1}H NMR chemical shift of the corresponding proton is observed with reasonably good correlation coefficient following the equation: R(H-bond) = 321.62 *$(\delta^1H)^{-0.328}$ (RMSD = 0.95) (Figure 5). Koller et al.[30] suggested a similar power relation, however, between the parameter "hydrogen bond valence" and ^{1}H NMR chemical shifts.

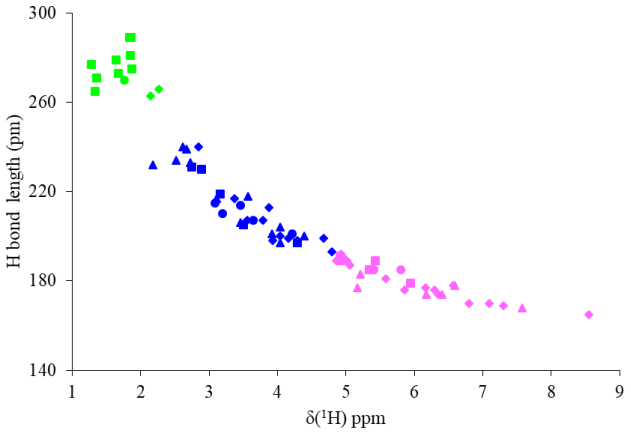

Figure 5. Plot of the hydrogen-bonded distance, R(H-bond), when the corresponding silanol group participates as proton-donor in a hydrogen bond and the ^{1}H NMR chemical shift of the corresponding proton in the nanoparticle models: ZNP-99 (squares), ZNP-111 (circles), ZNP-165 (triangles), ZNP-213 (rhombus). Tentative assignment of the data points corresponding to strong (pink), medium (blue), and weak (green) hydrogen bonds.

The R(H-bond) length versus the ^{1}H NMR chemical shift also shows clearly three different regions plotted in different colors in Figure 5. For the purpose of the hydrogen bonds in silanol groups, those three regions may be considered to correspond to strong, medium and weak hydrogen bonds (note that this may differ from earlier classifications applied for molecular systems).[1,2] The border values for the corresponding types of hydrogen bonds, determined on the base of the R(H-bond)/^{1}H NMR chemical shift intervals, are shown in Table S3 and the corresponding data for O-H vibrational frequencies and O-H distances are plotted in Figure S3.

The comparison of the structural features of different silanols and their experimental spectra suggests that the main factor determining both O-H stretching frequency, ν(O-H), of the silanols group and the ^{1}H NMR chemical shift, δ^1H, of the protons is the participation of that silanol in hydrogen bond as proton-donor, which leads to elongation of the O-H bond. Based on this observation we may consider different types of silanols (Table S3):

a. Isolated (free) silanols: they do not participate in hydrogen bonds either as proton-donors nor as proton-acceptors. Their typical R(O-H) bond length is in the ranges 96.1 – 96.3 pm, the O-H stretching frequencies is in the range 3745 – 3702 cm^{-1}, and the proton chemical shift is in the range 1.27 – 1.96. The O-H distance in the isolated reference molecule trimethylsilanol, $(CH_3)_3SiOH$ (R(O-H) = 96.1 pm), is similarly calculated, and its experimental O-H stretching frequency falls also in this range, 3735 cm^{-1}.

b. Proton-acceptor silanols: they participate in hydrogen bonds only as proton-acceptor with the following characteristic parameters: R(O-H) bond length of 96.1 – 96.6 pm, O-H stretching frequencies of 3737 – 3676 cm^{-1}, and proton chemical shift of 1.38 – 2.26 ppm.

c. Proton-donor silanols in weak hydrogen bonds: they have the following characteristic distances and spectral parameters: R(O-H) bond length of 96.1 – 96.6 pm, O-H stretching frequencies of 3745 – 3677 cm^{-1}, proton chemical shift of 1.27 – 2.28 ppm, and the H-bond distance is above 260 pm.

d. Medium and strong hydrogen bonded silanols as proton-donors or simultaneously as proton-donors and proton-acceptors characterized by a ^{1}H NMR chemical shift and O-H vibrational frequency ranges between 2.64 – 4.63 ppm and 3670 – 3454 cm^{-1} respectively. While for the strong hydrogen bonds the ranges are 4.83 – 8.44 ppm and 3500 – 3100 cm^{-1}.

The calculated characteristics of the first three groups of silanols suggest substantial overlap of their O-H stretching frequencies and the corresponding protons' chemical shifts. Thus, based on those intervals of O-H vibrational frequencies and ^{1}H NMR chemical shifts one may not distinguish between those types of silanols. This is clearly seen in Table S3 and Figure S3 (upper part of panel C) where the points corresponding to isolated silanols and proton-acceptor silanols are observed in the same area.

All four types of hydroxyls and corresponding protons are observed in the experimental spectra of the three zeolite samples synthesized. Interestingly, they do not have the same proportion when the size of the particle changes as shown in Figure 2. The proportion that corresponds to each type of silanols is listed in Table S1, SI. This opens the door for zeolite properties engineering through defect tuning.

As already reported, with increasing the strength of the hydrogen bond as proton-donor, the O-H bond length and the ^{1}H NMR chemical shift of the corresponding silanol increases, while O-H vibrational frequency decreases. One may assume that the medium hydrogen bonds are formed when the silanol participate only as proton-donor, while the strong hydrogen bonds correspond to silanols, participating in hydrogen bonds both as proton-donors and proton-acceptor. This assumption, however, is not justified, as shown in panel C of Figure S3. The blue circles and violet rhombus, corresponding to H-bond donor and acceptor silanols, and of H-bond proton-donors silanols, respectively, are located almost uniformly in the regions assigned to medium and strong hydrogen bonds. Only in the region of strongest hydrogen bonds, above 6.0 ppm, the silanols participating in hydrogen bonds as both proton donors and acceptors dominate. Thus, the main factor determining the strength of the hydrogen bond of a specific silanol group is the possibility its proton to approach closer the oxygen center of the proton accepting silanol. This suggests that the flexibility of the zeolite fragment at which the proton-donating and proton-accepting silanols are bound is the main factor determining the formation and strength of the hydrogen bonds, as well as the corresponding spectral features. In some of the models we considered deprotonated hydroxyl groups, one may observe also very strong hydrogen bonds directed towards the oxygen center from the deprotonated group. According to the computational results, such hydrogen bond is shorter than 170 pm, R(O-H) bond length is longer than 100 pm, O-H stretching frequency is lower than 3000 cm^{-1}, and the ^{1}H NMR chemical shift of the protons is around or higher than 10 ppm. Since the experimentally studied zeolite nanoparticles are neutral and do not contain deprotonated silanols, such features are not observed in the IR and NMR spectra, shown in Figure 2. However, similar values of the ^{1}H NMR chemical shift have been observed in alkaline glasses or zeolites containing charge defects.[20,31,32]

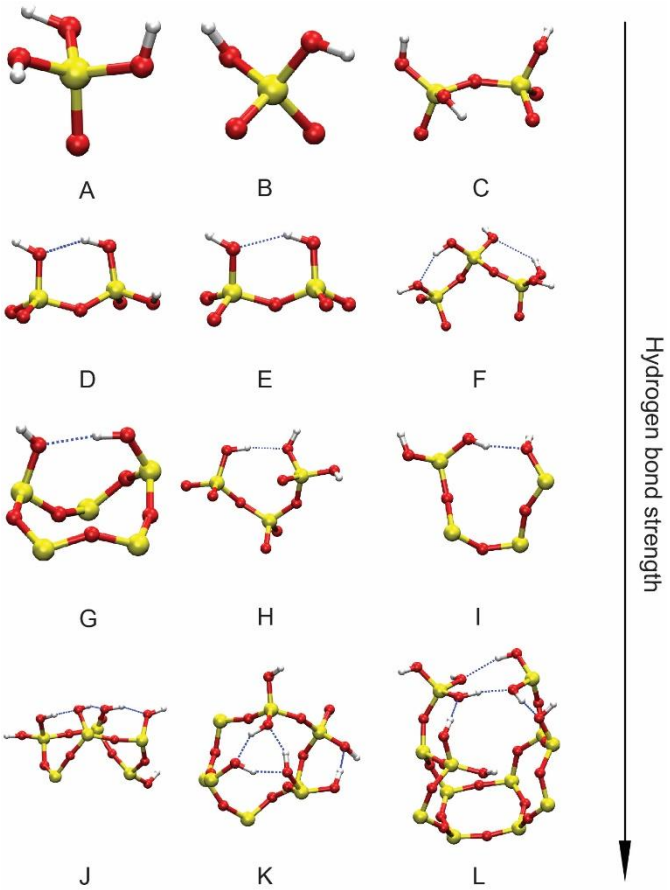

Figure 6. Selected fragments from the modelled zeolite nanoparticle showing different types of silanols and hydrogen bonds between them.

The variety of structural fragments in the modeled zeolite nanoparticles allowed us to analyze some specific types of silanols that may exist in the real zeolite samples. Earlier works suggested that geminal silanol groups, i.e. two hydroxyl groups at one silicon centers form hydrogen bonds between themselves. The orientation of such hydroxyl groups, however, does not allow formation of hydrogen bond between them (Figure 6A, B). Each of the hydroxyls may participate in hydrogen bonds with silanols bound to other silicon centers (Figure 6D). Since the whole $Si(OH)_2$ fragment, containing geminal silanols, is bound to the rest of the zeolite moiety via two Si-O-Si bonds, it is more mobile than Q^3 type silicon, which allows the former to approach closer neighboring silanols. When the hydroxyl groups are located at neighboring silicon centers, i.e. vicinal silanols, the formation of the hydrogen bond between them depends on the orientation of the oxygen centers between the silicon centers. If the oxygen center is

oriented in the same direction as the two hydroxyls (Figure 6C), hydrogen bond between them cannot be formed. However, when the oxygen center is oriented to the opposite direction, then hydrogen bond is formed in most cases with medium strength (Figure 6D-F). Most of the observed hydrogen bonds, either medium or strong, are formed between hydroxyl groups bound to next nearest neighbor or farther silicon centers (Figure 6G-I). As mentioned above, this can be accomplished if the silanol groups and the silicon centers, where they are bound, are sufficiently mobile. Common features in some of the modeled zeolite nanoparticles are networks of hydrogen bonded silanols – chains of subsequently bonded silanols or silanol nests (Figure 6J-L), as well as combination of those networks. Most of the silanols in such hydrogen bonded networks participate both as proton donors and proton acceptors and their spectral features correspond to strong hydrogen bonded silanols.

In summary, the interpretation of ^{1}H NMR spectra and the OH stretching region in IR spectra even of pure silica zeolites is not straightforward. The silanols exhibit a very complex hydrogen bonded network even in the pure silica zeolites (silicalite-1) that varies with the size of the crystals synthesized. The bigger the size of the zeolite nanocrystals, the higher the total concentration of silanols is measured. However the isolated silanols are favoured in the crystals with decreasing of particle size. To reveal the enigma we used computational modelling based on density functional theory. This allowed us to assign the experimental spectral features to specific structures and interactions of the silanol groups in the zeolite nanoparticles. A new classification of silanols based on their specific spectral behaviour and participation in hydrogen bonds is suggested: (i) isolated (free) silanols that do not participate in hydrogen bonds either as proton-donors nor as proton-acceptors, (ii) proton-acceptor silanols that include silanols participating in hydrogen bonds only as proton-acceptor; (iii) proton-donor silanols participating in weak hydrogen bonds; and (iv) medium and strong hydrogen bonded silanols as proton-donors or simultaneously as proton-donors and proton-acceptors. We have shown that the geminal or vicinal silanols cannot be distinguished from others based on their spectral features since their participation in hydrogen bonds is determined by the presence of neighbouring proton accepting centres. The general conclusion is that the main factor determining the formation and strength of the hydrogen bonds between silanols, as well as the corresponding spectral behaviour, is the flexibility of the zeolite fragment at which the proton-donating and proton-accepting silanols are bound.

Based on computational modeling we found several correlations between geometrical parameters of the silanol groups and their spectral characteristics. The simple numerical relations reported here may be useful for tentative calculation of the R(O-H) bond length from the measured vibrational frequency of a silanol or from the ^{1}H NMR chemical shift of the proton. With the derived linear correlations, one may also predict the value of the O-H stretching frequency from the measured ^{1}H NMR chemical shift and vice versa.

Acknowledgments

GNV and HAA acknowledge the support of the project EXTREME, funded by the Bulgarian Ministry of Education and Science (D01-76/30.03.2021), and computational resources provided by the European Regional Development Fund within the Operational Programme "Science and Education for Smart Growth 2014 - 2020" under the Project CoE "National center of mechatronics and clean technologies" BG05M2OP001-1.001-0008". ED, ICM and SM are grateful for the support by TOTAL and the Industrial Chair ANR-TOTAL “Nano Clean Energy” and Normandy University, and the Lable of Excellence for the Centre of Zeolites and Related Nanoporous Materials by the Region of Normandy.

Conflicts of interest

There are no conflicts to declare.

Notes and references

1 G. A. Jeffrey, An introduction to Hydrogen Bonding, Oxford University Press, Oxford, 1997.
2 T. Steiner, *Angew. Chem. Int. Ed*. 2002, **41**, 48-76.
3 L. B. McCusker, *Science*, 2017, **355**, (6321), 136.
4 G. A. Jeffrey, Y. Yeon, *Acta Cryst.*, 1986, **B42**, 410-413.
5 E. Brunner, H. G. Karge and H. Pfeifer, *Zei. Phys. Chem*. 1992, **176**, 173-183.
6 K. Hadjiivanov, *Advances in Catalysis*, Fr. C. Jentoft (Ed.) Academic Press, 2014, **57**, 99-318.
7 G. Paul; C. Bisio; I. Braschi; M. Cossi; G. Gatti; E. Gianotti; L. Marchese, *Chemical Society Reviews*, 2018, **47**, 5684-5739.
8 M. Guisnet, J.-P. Gilson, Zeolites for Cleaner Technologies, 2005, Imperial College Press, ISBN: 1860943292.
9 S. Mintova, J.-P. Gilson, V. Valtchev, *Nanoscale*, 2013, **5**, 6693-6703.
10 A.B. Pinar, C. Márquez-Álvarez, M. Grande-Casas, J. Pérez-Pariente, *Journal of Catalysis*, 2009, **263**, (2), 258–265.
11 A. W. Burton, S. I. Zones, S. Elomari, *Current Opinion in Colloid & Interface Science*, 2005, **10**, (5–6), 211–219.
12 L. Zhang, K. Chen, B. Chen, J. L. White and D. E. Resasco, *J. Am. Chem. Soc.* 2015, **137**, (36), 11810–11819.
13 E. Dib, T. Mineva, E. Veron, V. Sarou-Kanian, F. Fayon and B. Alonso, *J. Phys. Chem. Lett*. 2018, **9**, 19–24.
14 U. Fleischer, W. Kutzelnigg, A. Bleiber, J. Sauer, *J. Am. Chem. Soc*. 1993, **115**, (17), 7833–7838.
15 R. A. van Santen and G. J. Kramer, *Chem. Rev.* 1995, **95**, (3), 637–660.
16 P. Concepción, M. Boronat, R. Millán, M. Moliner, A. Corma, *Top Catal*, 2017, **60**, 1653–1663.
17 A. Jones and E. Iglesia, *ACS Catalysis*, 2015, **5**, 5741-5755.
18 L. Treps, C. Demaret, D. Wisser, D. Harbuzaru, A. Methivier, E. Guillon, D. V. Benedis, A. Gomez, T. de Bruin, M. Rivallan, L. Catita. A. Lesage, C. Chizalet, *J. Phys. Chem. C*. 2021, **125**, (3), 2163–2181.
19 C. Schroeder, V. Siozios, C. Mück-Lichtenfeld, M. Hunger, M. R. Hansen, H. Koller, *Chem. Mater*, 2020, **32**, 1564-1574.
20 C. Schroeder, V. Siozios, M. Hunger, M. R. Hansen and H. Koller, *J. Phys. Chem. C* 2020, **124**, 23380-23386.
21 A. Lesage, D. Sakellariou, S. Hediger, B. Eléna, P. Charmont, S. Steuernagel, L. Emsley, *J. Magn. Res*., 2003, **163**, (1), 105-113.
22 S. Bordiga, C. Lamberti, F. Bonino, A. Travert and F. Thibault-Starzyk, *Chem. Soc. Rev*., **2015**, 44, 7262-7341.
23 http://www.iza-structure.org/databases.

24 G. Busca, Heterogeneous Catalytic Materials. Solid State Chemistry, Surface Chemistry and Catalytic Behaviour, 1st edition, Elsevier, Amsterdam, 2014, p. 155.
25 W. Chassé, J. L. Valentín, G. D. Genesky, C. Cohen, K. Saalwächter, *J. Chem. Phys.* 2011, **134**, 044907.
26 F. Neese, Wiley *Interdiscip. Rev.: Comput. Mol. Sci*., 2012, **2**, 73-78.
27 F. Neese, *Wiley Interdiscip. Rev. Comput. Mol. Sci.*, 2017, **8**, e1327.
28 E. Brunner, *J. Molec. Struc.* 1995, **355**, 61-85.
29 J. Rouviere, V. Tabacik, G. Fleury, *Spectrochim. Acta A*, 1973, **29**, 229-242.
30 H. Koller and M. Weiss, *Top. Curr. Chem*., 2012, **306**, 189–228.
31 H. Koller, R. F. Lobo, S. L. Burkett, M. E. Davis, *J. Phys. Chem*., 1995, **99**, 12588–12596.
32 E. Dib, J. Grand, S. Mintova, C. Fernandez, *Chem. Mater*., 2015, **27**, 7577–7579.